Periodic Stepped-Impedance Ring Resonator (PSIRR) Bandpass Filter With a Miniaturized Area and Desirable Upper Stopband Characteristics

Jen-Tsai Kuo, *Senior Member, IEEE,* and Chih-Yuan Tsai

***Abstract*—A periodic stepped-impedance ring resonator (PSIRR) is proposed to design dual-mode bandpass filters with a miniaturized area and desirable upper stopband characteristics. Design parameters of a PSIRR include impedance ratio R of the hi-Z to low-Z sections, their lengths, and number of impedance steps $2N$. The resonant characteristics of PSIRRs with various N and R values are investigated by both the transmission-line theory and electromagnetic simulation. Proper choice of the above parameters leads to an optimal reduction of circuit area and extension of upper rejection bandwidth. Two extra transmission zeros exist in the upper stopband and are tunable via changing the arm lengths of the line-to-ring coupling structure. Realized by the standard microstrip technology, the dual-mode PSIRR bandpass filter has not only the first spurious response at higher than 3.7× the passband frequency, but also an area reduction of better than 60% against a conventional ring filter. Experimental results of several fabricated circuits validate the analysis and theoretical prediction.**

***Index Terms*—Bandpass filter, dual mode, miniaturization, periodic structure, ring resonator, stepped-impedance resonator.**

I. Introduction

HIGH-PERFORMANCE microwave/RF bandpass filters are essential devices in modern wireless communications such as satellite and mobile systems. The dual-mode ring resonator filters have many attractive features such as small area, low loss, high selectivity, and simple design. Recently, many researches on ring filters have been published for innovative design or analysis methods [1]–[4], circuit miniaturization [5]–[8], and wide stopband properties [9]–[11]. In [1], L-shaped arms are used to enhance couplings and dual-mode excitations of quasi-elliptic function bandpass filters. Based on the transmission-line theory, the even- and odd-mode method in [2] is now popular for analysis of a dual-mode ring resonator possessing two ports spatially separated at 90° and an impedance junction for perturbation at its symmetrical plane. In [3], the angle between the I/O ports and the coupling between the dual modes are combined in formulation to control the attenuation pole frequencies. In [4], a joint field/circuit model is proposed to characterize line-to-ring coupling structures for design and optimization of microstrip ring resonator circuits.

Recently, several structures have been developed for reducing area of a dual-mode ring filter. The meander loop in [5] has a size reduction of more than 50%. In [6], a sophisticated pattern is designed for the dual-mode resonator to achieve a size reduction of 59%. In [7], a miniaturized ring filter is designed with four equally spaced butterfly radial stubs. A new perturbation, called the local ground defect, is included to make the orthogonal modes split up. A size reduction of better than 65% can be obtained. The etched holes in the ground plane, however, need extra fabrication efforts. In [8], two pairs of shunt capacitors are used to control the even and odd resonances for perturbation. A size reduction of 55% $\sim$ 67% is realized. Note that their circuits involve lumped capacitors and via-holes.

Planar or quasi-planar bandpass filters suffer from unwanted responses in the upper stopband due to the distributed nature and other circuit properties. For widening the upper stopband, slow-wave open-loop resonators are embedded into a square loop resonator [9]. The spurious is detected at 2.5× the design frequency. In [10], two topologies are proposed to suppress the unwanted harmonics. One intuitively connects 50-Ω spur-line bandstop filters at the I/O ports, and the other incorporates low-pass structures into the ring. The ring in [11] increases the rejection bandwidth by directly incorporating a stepped-impedance low-pass filter to suppress the second mode.

In this paper, we propose a new fully planar microstrip periodic stepped-impedance ring resonator (PSIRR) bandpass filter. The design utilizes degenerate modes of a ring resonator consisting of a periodic cascade of hi-Z and low-Z sections. The proposed PSIRR has a compact area and a wide upper stopband with two extra transmission zeros. One of the zero can be tuned to suppress the first spurious so that the upper stopband can be extended up to 3.76× the passband frequency.

II. PSIRR

Fig. 1 shows layouts of the proposed PSIRRs of $N = 1$–4. Each PSIRR consists of N hi-Z sections of a spatial angle $2\theta_1$. Every two adjacent hi-Z sections are spaced by a low-Z section of a spatial angle $2\theta_2$. All PSIRRs are symmetric about at least one dashed line so that $\theta_1 + \theta_2 = \pi/N$. Such a PSIRR is herein referred to as PSIRRN. For example, a PSIRR with $N = 3$ is

Manuscript received June 20, 2005; revised November 1, 2005. This work was supported in part by the National Science Council, Taiwan, R.O.C., under Grant NSC 93-2213-E-009-095 and Grant NSC 93-2752-E-009-002-PAE.

The authors are with the Department of Communication Engineering, National Chiao Tung University, Hsinchu 300, Taiwan, R.O.C. (e-mail: jtkuo@cc.nctu.edu.tw).

Digital Object Identifier 10.1109/TMTT.2005.864121

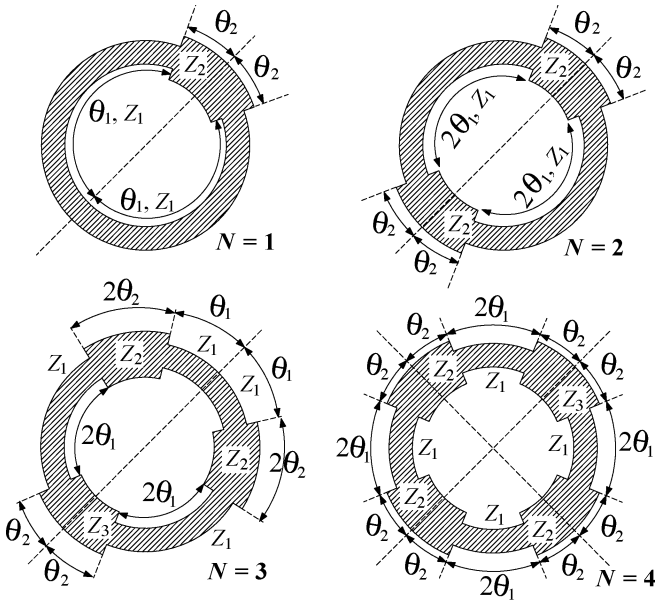

Fig. 1. Layouts of the proposed PSIRRs for $N = 1, 2, 3$, and 4. $\theta_1 + \theta_2 = \pi/N$.

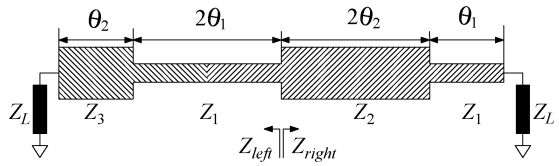

Fig. 2. Transmission-line modeling of a PSIRR3. In analysis, $Z_L = 0$ and ∞ for the odd and even modes, respectively.

denoted as PSIRR3. When $N \geq 3$, the Z_3-section is a perturbation of the Z_2-section to split off the degenerate modes. Define the impedance ratios of a PSIRR as

$$R = \frac{Z_1}{Z_2} \geq 1 \tag{1a}$$

$$R' = \frac{Z_1}{Z_3} \geq 1 \tag{1b}$$

where R'/R is close to unity and R' is used only for $N \geq 3$.

The resonant conditions for the PSIRRs can be formulated by the transmission-line theory [2]. For example, the PSIRR3 can be modeled by the multistepped-impedance lines with terminations Z_L shown in Fig. 2. The odd and even resonances of the PSIRR3 occur when $Z_L = 0$ and ∞, respectively. Thus, the resonant condition for the odd mode can be formulated by enforcing the sum of the following two terms to zero:

$$Z_{\text{left}} = jZ_1 \frac{Z_3 \tan\theta_2^e + Z_1 \tan 2\theta_1^e}{Z_1 - Z_3 \tan 2\theta_1^e \tan\theta_2^e} \tag{2a}$$

$$Z_{\text{right}} = jZ_2 \frac{Z_1 \tan\theta_1^e + Z_2 \tan 2\theta_2^e}{Z_2 - Z_1 \tan\theta_1^e \tan 2\theta_2^e} \tag{2b}$$

where Z_{right} and Z_{left} are the input impedances seen at the $Z_1 - Z_2$ junction looking to the right- and left-hand sides, and θ_1^e and θ_2^e are electrical lengths of spatial angles θ_1 and θ_2, respectively.

Based on (2a) and (2b), a simple root-searching program can be employed to calculate the resonant frequencies as functions of R, R', θ_1, and θ_2. Fig. 3 plots the leading two resonant frequencies for PSIRRs with $N = 1, 2, \ldots, 8$ against θ_2 from

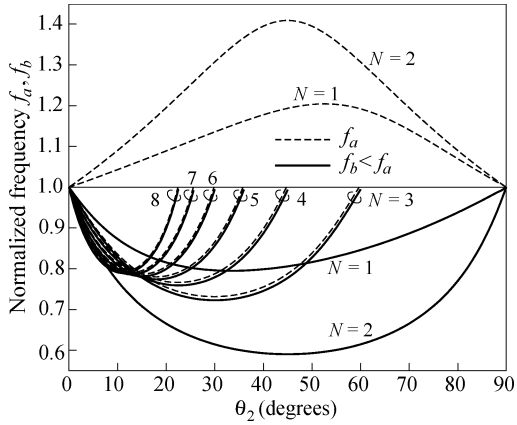

Fig. 3. Normalized resonant frequencies of perturbed PSIRRs for $N = 1, 2, \ldots, 8$. All rings have identical radii. Impedance ratios $R = 4$ and $R' = 1.04 \times R$.

TABLE I
MINIMAL NORMALIZED FREQUENCIES f_a FOR PSIRR3 AND PSIRR4

R	2.5	3	3.5	4	4.5	5
$N = 3$	0.8511	0.8098	0.7677	0.7316	0.6958	0.6700
$N = 4$	0.8825	0.8392	0.8003	0.7666	0.7346	0.7069

0 to $\min(\pi/2, \pi/N)$ for $R = 4$ and $R' = 1.04 \times R$. The plotted frequencies are normalized with respect to the fundamental frequency of a uniform impedance ring (UIR) resonator, i.e., $Z_1 = Z_2 = Z_3$. Here, all the PSIRRs have identical mean radii. When miniaturization is the design target, the desired resonator will have a frequency as low as possible. As indicated in Fig. 3, PSIRR2 has the lowest resonant frequency. Its second resonance, however, is far away from the previous one due to the large R value. Note that the design frequency of a dual-mode ring filter should be the algebraic mean of these two resonances. The large distance between the two resonances will lead to a large bandwidth, but at the same time, very large couplings between feeders and the ring can be inevitable. Thus, PSIRR2 is not suitable to our purpose, while PSIRR3 becomes the best candidate.

III. RESONATOR MINIATURIZATION AND THE UPPER STOPBAND

For PSIRRs with $N \geq 3$, as shown in Fig. 3, the two resonant frequencies f_a and f_b splitting up from the degenerate frequency f_1 have a small distance in response to the 4% change of Z_2 to Z_3. Our simulation shows that $f_b < f_a \approx f_1$. When θ_2 is varied from 0° to 90°, each PSIRR has a minimal f_a. Detailed data show that the minimal f_a locate at $\theta_1 = \theta_2 = \pi/2N$.

Table I lists the minimal frequencies f_a of the PSIRR3 and PSIRR4 for $2.5 \leq R \leq 5$. As compared with a UIR resonator, the PSIRR3 with $R = 4.5$ will use only $(0.6958)^2 = 48.4\%$ area, i.e., an area reduction of 51.6% can be achieved. When $R = 4$, the f_a value for $N = 4$ is approximately 4.8% higher than that for $N = 3$ and those for $N = 5$–8 gradually increase from 0.78 to 0.793. Based on Table I, the area can be effectively reduced by increasing the R value; however, parasitic effects will also contribute further area reduction, which will be shown below.

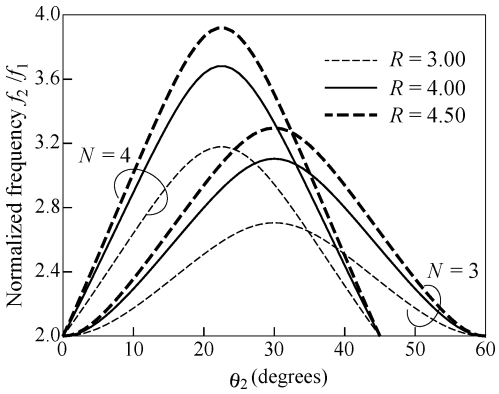

Fig. 4. Ratios of the first higher order resonant frequency to the fundamental resonance for the PSIRR3 and PSIRR4.

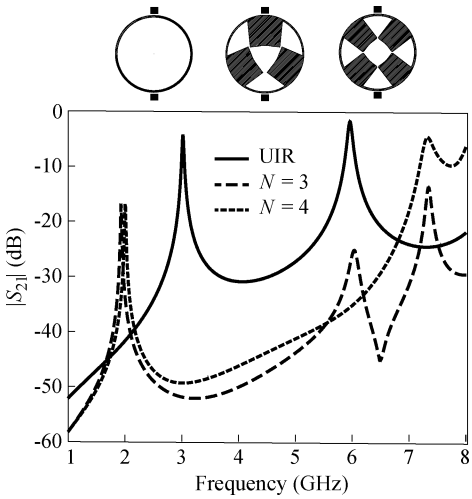

Fig. 5. EM simulation results for the normalized fundamental and first higher order resonant frequencies of the PSIRR3 and PSIRR4.

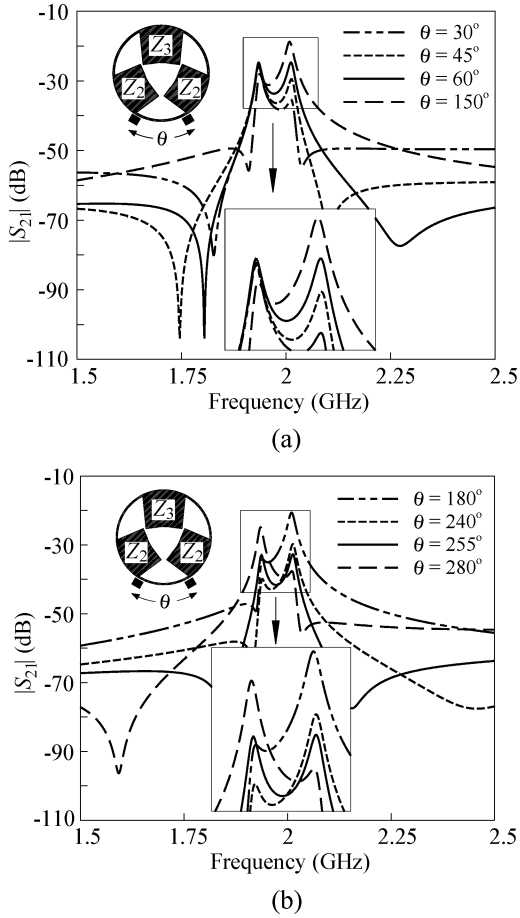

Fig. 6. Search for spatial separation θ between I/O feeders for a PSIRR3. (a) $\theta = 30°, 45°, 60°, 150°$. (b) $\theta = 180°, 240°, 255°, 280°$.

It is also desirable for a distributed bandpass filter to have a wide upper stopband. The performance of the filter in the upper stopband depends much on where the second resonance f_2 arises. Fig. 4 plots f_2/f_1 against θ_2 for PSIRR3 and PSIRR4. It is found that the θ_2 for maximal f_2/f_1 are the same as those for minimal f_1. It means that choosing $\theta_1 = \theta_2$ for a PSIRR will have a minimal ring area and maximally possible upper stopband at the same time.

Fig. 5 compares the simulated resonant spectrum of a PSIRR3 and PSIRR4 for $R = 4.5$ with that of a UIR on a dielectric substrate with $\varepsilon_r = 10.2$ and thickness $= 1.27$ mm. The simulation data are obtained by the electromagnetic (EM) software package IE3D.[1] All rings have identical radii $r = 6.27$ mm, measured from the ring center to midpoint of the hi-Z line. This size will be used for all PSIRR filters herein. The feed lines are separated from the ring by a coupling gap so that resonant frequencies can be easily located at the sharp peaks. It can be verified that the UIR circuit has $f_1 = 3$ GHz. The PSIRR3 and PSIRR4 have fundamental resonances at 1.93 and 1.98 GHz, corresponding to normalized frequencies 0.643 and 0.660, respectively. These two values are $7\% \sim 10\%$ less than those given in Table I and Fig. 3. This discrepancy should be resulted from the parasitic effects due to the $2N$ step discontinuities of the ring, which are not taken into account in the transmission-line analysis.

For the particular I/O arrangement, the first higher order resonance of the UIR is at $2f_1 = 6$ GHz, while those of the PSIRR3 and PSIRR4 are at 6.04 and 7.35 GHz, respectively. For the PSIRR4, if the I/O feeds are taken collinearly passing through the low-Z sections, there is a higher order resonance at 2.9 GHz and that at 7.35 GHz disappears at the same time. The former can be predicted by merely interchanging the roles of hi-Z and low-Z sections in (2), and the latter is attributed to a longitudinal resonance in the low-Z section, at which there is a field minimum.

Miniaturization of resonators is usually accompanied with increase of losses. Insertion of the simulated peak responses in Fig. 5 to the formula in [12] yields the unloaded Q factors of PSIRR3 and PSIRR4 $Q_o = 135$, which is comparable to $Q_o = 145$ for a uniform microstrip ring with a 50-Ω linewidth.

IV. Dual-Mode Ring Resonator Filter Design

The purpose for R' being made slightly larger than R is to produce a proper coupling between the two degenerate modes.

[1]IE3D Simulator, Zeland Software Inc., Fremont, CA, 1997.

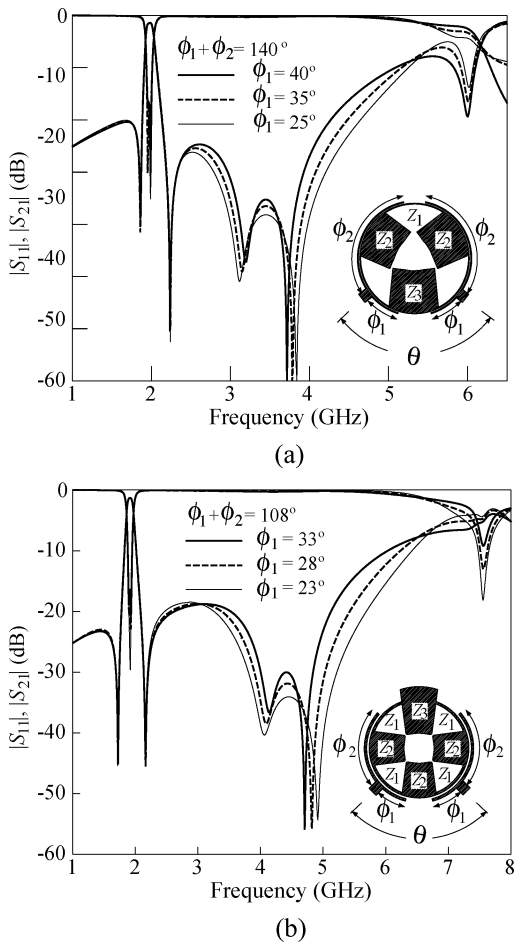

Fig. 7. Tuning of the two transmission zeros in the upper stopband for two PSIRR filters. (a) $N = 3$ and $\theta = 60°$. (b) $N = 4$ and $\theta = 90°$.

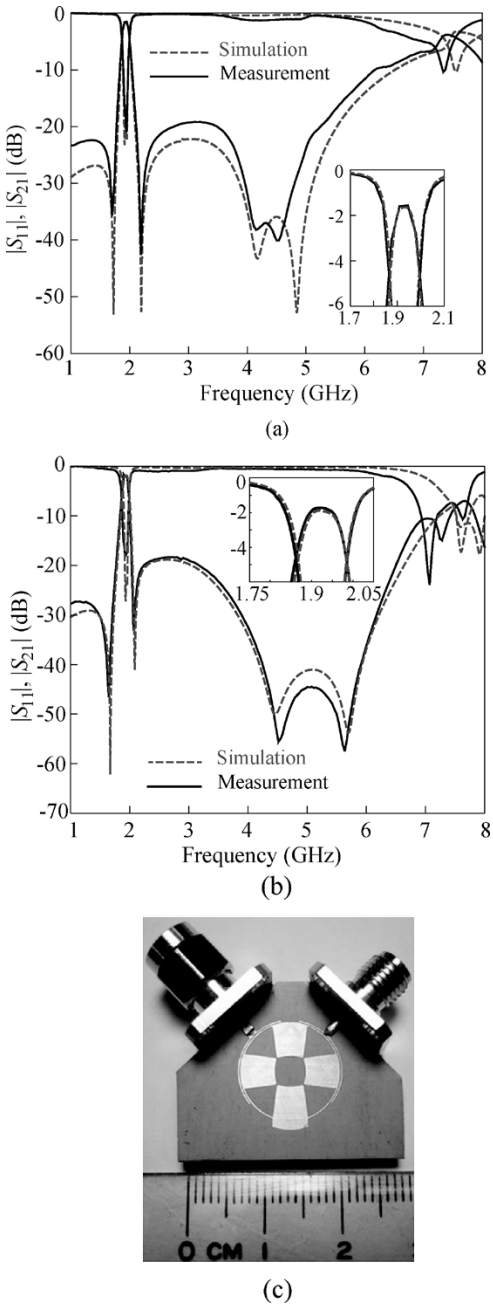

Fig. 8. Simulation and measured responses for two PSIRR4 filters. $R = 4.5$. (a) $\phi_1 = 30°$, $\phi_2 = 80°$, $\theta = 90°$ [see Fig. 7(b)], $R' = 5.3$. (b) $\phi_1 = 90°$, $\phi_2 = 10°$, $\theta = 275°$, $R' = 5.15$. (c) Photograph of circuit in (a).

This perturbation is similar to the conventional patch perturbation in [2], [5], [6], and [8]. The coupling coefficient between the two modes in a PSIRR can be calculated as [2], [3], [8]

$$C = 2\frac{|f_a - f_b|}{f_a + f_b} \tag{3}$$

where f_a and f_b are the $|S_{21}|$ peak frequencies. Note that f_a and f_b are consistent with those used in Fig. 3. Comparing (3) with [1, eq. (3)], one can easily validate that their relative deviation is $C^2/4$. For example, if $C \leq 8\%$, their relative deviation will be no larger than 0.0016.

For a dual-mode ring resonator filter, the feeders should be properly designed for a symmetric passband response. Fig. 6 plots the $|S_{21}|$ responses for a PISRR3 having $R = 4.2$ and $R' = 4.6$ with various separations θ between the feeders, which is symmetric about the vertical axis through center of the ring and has a small coupling gap to the ring. Two separations $\theta = 60°$ and 255° are found to equalize the $|S_{21}|$ peaks at f_a and f_b. For a PSIRR4, with the perturbation section being symmetrically located at vertical axis above the center of the ring, identical $|S_{21}|$ peaks are obtained when $\theta = 90°$ and 275°.

The peak $|S_{21}|$ levels for $\theta = 60°$ in Fig. 6(a) is approximately 7 dB higher than that for $\theta = 255°$ in Fig. 6(b). It means that the latter will need more I/O couplings than the former for a given filter bandwidth. To establish the necessary couplings between the dual-mode resonator and the feeders, the line-to-ring coupling structure [4] is used herein.

Both the PSIRR3 and PSIRR4 filters are found to have two extra zeros in the upper stopband before the first spurious arises. These zeros are desirable since they greatly improve the rejection in the upper stopband. The generation of the two zeros depends on the structure and position of the line-to-ring feeder, separation of the I/O ports θ, and the PSIRR structure. Fig. 7(a) and (b) plots the simulation responses of the PSIRR3 and PSIRR4 filters when the feeders have total arc lengths $\phi_1 + \phi_2 = 140°$ and 108° and $\theta = 60°$ and 90°, respectively. Here, $R = 4.13$ and $R' = 4.57$. The coupling arms have a

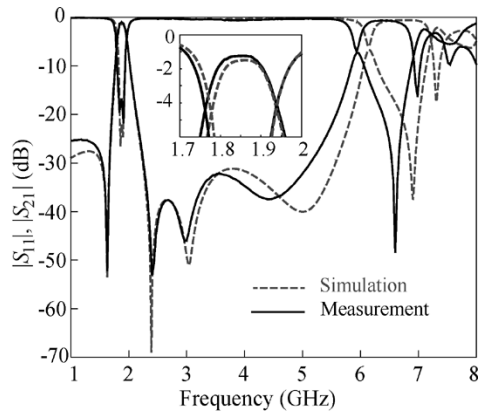

(a)

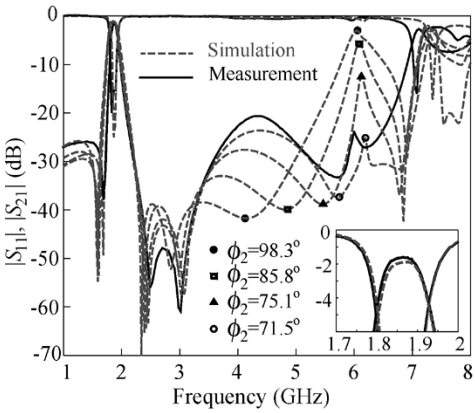

(b)

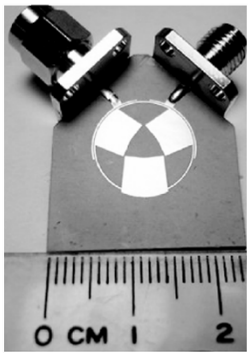

(c)

Fig. 9. Simulated and measured responses for two PSIRR3 filters. Center frequency $f_o = 1.86$ GHz. (a) $\phi_1 = 17°$, $\phi_2 = 93°$, $\theta = 8\%$, measured $f_o = 1.85$ GHz. (b) Tuning ϕ_1 and ϕ_2 to have spurious suppression at 6 GHz. (c) Photograph of circuit in (a).

width and a gap of 0.14 mm from the ring. In Fig. 7(a), when ϕ_1 is decreased from 40° to 25°, the distance between the two zeros increases. Similar results are obtained when ϕ_1 is decreased from 33° to 23° for the PSIRR4 filter. Note that the passband responses are close to not being altered when ϕ_1 is changed. These results indicate that the two zeros are tunable to a certain extent via adjusting ϕ_1.

V. Simulation and Measurements

Four PSIRR filters are fabricated on a substrate with $\varepsilon_r = 10.2$ and thickness $= 1.27$ mm. The circuits are measured by the HP8722D network analyzer, and the standard short-open-load-thru (SOLT) calibration is used. The dimensions of the experimental circuits are chosen as follows. As in Table I, the larger the R value, the more the area reduction. A large R value, however, corresponds to a large low-Z patch. Thus, R is made as large as possible, but to avoid overlapping the low-Z sections inside the ring. The value of R' determines the filter bandwidth, the I/O separation θ is based on the results in Fig. 6, and the choices of θ_1 and θ_2 are from those in Fig. 7.

Fig. 8(a) and (b) shows the results for two PSIRR4 filters with $\theta = 90°$ and 275°, respectively. The center frequency $f_o = 1.93$ GHz. It implies that they need only $(1.93/3)^2 = 41.4\%$ of the area of a traditional ring filter. In Fig. 8(a), the PSIRR4 has $Z_1 = 102.5\ \Omega$, $Z_2 = 22.78\ \Omega$, and $Z_3 = 19.47\ \Omega$, and the measured bandwidth 6.25%. The feeder has $\phi_1 = 30°$ and $\phi_2 = 80°$. In Fig. 8(b), the PSIRR4 is a duplicate of the previous one, except $Z_3 = 19.88\ \Omega$. Its bandwidth is 4.5%. The feeder has $\phi_1 = 90°$ and $\phi_2 = 10°$ to increase the separation between the two zeros. Both filters in Fig. 8 have in-band insertion losses of 1.7 dB and return losses close to 20 dB. The spurious of the two circuits are at 7.3 GHz or $3.78 f_o$, as well predicted by Fig. 5.

Fig. 9(a) plots the simulation and measured results of a PSIRR3 filter. The values of Z_1 and Z_2 are identical to those used in Fig. 8(a), but $Z_3 = 19.18\ \Omega$. The I/O port separation $\theta = 60°$, and lengths of the feeders' arms $\phi_1 = 17°$ and $\phi_2 = 93°$. In measurement, passband center $f_o = 1.85$ GHz, bandwidth $\Delta = 8\%$, and in-band insertion loss is 1.24 dB. The circuit occupies only 38% of the area of a traditional dual-mode ring filter at the same f_o. The spurious is at 6 GHz or $3.24 f_o$.

Fig. 9(b) plots the results of the second PSIRR3 filter. The circuit is the same as that in Fig. 9(a) with Z_3 being changed to 19.88 Ω. With $\phi_1 = 17°$, the distance ϕ_2 is swept from 100° to 70° to tune the notch at 5 GHz in Fig. 9(a). Simulated $|S_{21}|$ responses with $\phi_2 = 98.3°$, 85.8°, 75.1°, and 71.5° are plotted to show the migration of the notch. When $\phi_2 = 71.5°$, the notch cancels the spurious at 6 GHz so that the upper stopband has 1-GHz bandwidth extension for a 20-dB rejection level. This circuit is then fabricated and measured. The measured insertion loss in the passband is only 1.6 dB. The measurements have good agreement with the simulation.

VI. Conclusion

PSIRRs have been proposed for design of dual-mode ring bandpass filters. As compared with a traditional ring, PSIRR3 and PSIRR4 can offer a size reduction of approximately 60% for dual-mode filter design. The amount of size reduction depends on both the number of impedance junctions and impedance ratio of hi-Z to low-Z sections in a PSIRR. Two transmission zeros are generated in the upper stopband and are tunable by adjusting the arm lengths of the line-to-ring coupling structures. Measured results for two PSIRR3 and two PSIRR4 filters have been presented. For PSIRR3, one of the zeros can be used to suppress the first spurious and, hence, to extend the bandwidth of the upper stopband up to more than 3.7× the passband frequency.

REFERENCES

[1] L.-H. Hsieh and K. Chang, "Dual-mode quasi-elliptic-function bandpass filters using ring resonators with enhanced-coupling tuning stubs," *IEEE Trans. Microw. Theory Tech.*, vol. 50, no. 5, pp. 1340–1345, May 2002.

[2] M. Matsuo, H. Yabuki, and M. Makimoto, "Dual-mode stepped-impedance ring resonator for bandpass filter application," *IEEE Trans. Microw. Theory Tech.*, vol. 49, no. 7, pp. 1235–1240, Jul. 2001.

[3] A. C. Kundu and I. Awai, "Control of attenuation pole frequency of a dual-mode microstrip ring resonator bandpass filter," *IEEE Trans. Microw. Theory Tech.*, vol. 49, no. 6, pp. 1113–1117, Jun. 2001.

[4] L. Zhu and K. Wu, "A joint field/circuit model of line-to-ring coupling structures and its application to the design of microstrip dual-mode filters and ring resonator circuits," *IEEE Trans. Microw. Theory Tech.*, vol. 47, no. 10, pp. 1938–1948, Oct. 1999.

[5] J. S. Hong and M. J. Lancaster, "Microstrip bandpass filter using degenerate modes of a novel meander loop resonator," *IEEE Microw. Guided Wave Lett.*, vol. 5, no. 11, pp. 371–372, Nov. 1995.

[6] A. Görür, C. Karpuz, and M. Akpinar, "A reduced-size dual-mode bandpass filter with capacitively loaded open-loop arms," *IEEE Microw. Wireless Compon. Lett.*, vol. 13, no. 9, pp. 385–387, Sep. 2003.

[7] B. T. Tan, J. J. Yu, S. T. Chew, M. S. Leong, and B. L. Ooi, "A miniaturized dual-mode ring bandpass filter with a new perturbation," *IEEE Trans. Microw. Theory Tech.*, vol. 53, no. 1, pp. 343–348, Jan. 2005.

[8] M.-F. Lei and H. Wang, "An analysis of miniaturized dual-mode bandpass filter structure using shunt-capacitance perturbation," *IEEE Trans. Microw. Theory Tech.*, vol. 53, no. 3, pp. 861–867, Mar. 2005.

[9] A. Görür, "A novel dual-mode bandpass filter with wide stopband using the properties of microstrip open-loop resonator," *IEEE Microw. Wireless Compon. Lett.*, vol. 12, no. 10, pp. 386–388, Oct. 2002.

[10] U. Karacaoglu, D. Sanchez-Hernandez, I. D. Robertson, and M. Guglielmi, "Harmonic suppression in microstrip dual-mode ring-resonator bandpass filters," in *IEEE MTT-S Int. Microw. Symp. Dig.*, 1996, pp. 1635–1638.

[11] J. M. Carrol and K. Chang, "Microstrip mode suppression ring resonator," *Electron. Lett.*, vol. 30, no. 22, pp. 1861–1862, Oct. 1994.

[12] K. Chang, *Microwave Ring Circuits and Antennas*. New York: Wiley, 1996.

Jen-Tsai Kuo (S'88–M'92–SM'04) received the Ph.D. degree from the Institute of Electronics, National Chiao Tung University (NCTU), Hsinchu, Taiwan, R.O.C., in 1992.

Since 1984, he has been with the Department of Communication Engineering, NCTU, as a Lecturer in both the Microwave and Communication Electronics Laboratories. During the 1995 academic year, he was a Visiting Scholar with the University of California at Los Angeles (UCLA). He is currently a Professor and serves as the Vice Chairman of the Department of Communication Engineering and the Director of the Degree Program of the Electrical Engineering and Computer Science Colleges, NCTU. His research interests include the analysis and design of high-frequency electronics and microwave circuits, high-speed interconnects and packages, field-theoretical studies of guided waves, and numerical techniques in electromagnetics.

Chih-Yuan Tsai was born in Kaohsiung, Taiwan, R.O.C., on May 5, 1980. He received the B.S. degree in electrical engineering from National Taiwan Ocean University (NTOU), KeeLung, Taiwan, R.O.C., in 2003, and the M.S. degree in communication engineering from the National Chiao Tung University (NCTU), Hsinchu, Taiwan, R.O.C., in 2005.

His research interests include the analysis and design of passive microwave and millimeter-wave circuits, especially in development of innovative RF filters.